2 mid

NASA TECHNICAL NOTE **NASA TN D-7549**

NASA TN D-7549

ESTIMATION OF DEVIATION ANGLE FOR AXIAL-FLOW COMPRESSOR BLADE SECTIONS USING INVISCID-FLOW SOLUTIONS

by Max J. Miller

Lewis Research Center
Cleveland, Ohio 44135

NATIONAL AERONAUTICS AND SPACE ADMINISTRATION • WASHINGTON, D. C. • MARCH 1974

1. Report No. NASA TN D-7549	2. Government Accession No.	3. Recipient's Catalog No.
4. Title and Subtitle ESTIMATION OF DEVIATION ANGLE FOR AXIAL-FLOW COMPRESSOR BLADE SECTIONS USING INVISCID-FLOW SOLUTIONS		5. Report Date March 1974 6. Performing Organization Code
7. Author(s) Max J. Miller		8. Performing Organization Report No. E-7453
9. Performing Organization Name and Address Lewis Research Center National Aeronautics and Space Administration Cleveland, Ohio 44135		10. Work Unit No. 501-24 11. Contract or Grant No.
12. Sponsoring Agency Name and Address National Aeronautics and Space Administration Washington, D.C. 20546		13. Type of Report and Period Covered Technical Note 14. Sponsoring Agency Code

15. Supplementary Notes

16. Abstract

Development of a method of estimating deviation angles by analytical procedures was begun. Solutions for inviscid, irrotational flow in the blade-to-blade plane were obtained with a finite-difference calculation method. Deviation angles for a plane cascade with a rounded trailing edge were estimated by using the inviscid-flow solutions and three trailing-edge hypotheses. The estimated deviation angles were compared with existing experimental data over a range of incidence angles at inlet flow angles of 30° and 60°. The results indicate that deviation angles can be estimated accurately (within 1°) by using one of the three trailing-edge hypotheses, but only when pressure losses are low. A new trailing-edge hypothesis is presented which is suitable (for the cascade considered) for both low- and high-loss operating points.

17. Key Words (Suggested by Author(s))
Deviation angle
Axial compressor

18. Distribution Statement
Unclassified - unlimited

Cat. 01

19. Security Classif. (of this report)	20. Security Classif. (of this page)	21. No. of Pages	22. Price*
Unclassified	Unclassified	~~41~~ 43	~~$3.00~~ 3.25

* For sale by the National Technical Information Service, Springfield, Virginia 22151

ESTIMATION OF DEVIATION ANGLE FOR AXIAL-FLOW COMPRESSOR BLADE SECTIONS USING INVISCID-FLOW SOLUTIONS

by Max J. Miller*

Lewis Research Center

SUMMARY

Estimating the direction of the flow leaving a given annular cascade of blades over its operating range is an important problem in axial-flow turbomachinery aerodynamics. Herein, as for many compressor applications, the direction of the flow leaving a blade cascade has been predicted by estimating the difference between the average direction of leaving flow and the direction of the blade mean line at the trailing edge. This difference is defined as deviation angle. No completely satisfactory methods for estimating deviation angle are available.

The study reported herein considers estimating deviation angle for blade sections in a two-dimensional, subsonic flow by applying a currently available analytical procedure. Solutions for inviscid, irrotational flow in the blade-to-blade plane were obtained by a finite-difference calculation method. Deviation angles for a plane cascade with a rounded trailing edge were estimated by using the inviscid-flow solutions and three trailing-edge hypotheses. The estimated deviation angles were compared with existing experimental data over a range of incidence angles at inlet flow angles of 30° and 60°. The results indicate that deviation angles can be estimated accurately (within 1°) by using one of the three trailing-edge hypotheses, but only over the operating range where pressure losses are low. A new trailing-edge hypothesis is presented which is suitable (for the cascade considered) for both low- and high-loss operating points.

---

*The material presented in this report was included in the thesis submitted by the author to Iowa State University in partial fulfillment of the requirements for the degree doctor of philosophy in June 1973.

INTRODUCTION

Estimating the direction of the flow leaving an annular cascade of blades is an important problem in axial-flow turbomachinery aerodynamics. In design, blades must be selected which turn the fluid to the desired direction to achieve the desired energy transfer in rotors. Turning the flow to the desired direction is important in both rotors and stators because unexpected and unwanted losses can occur when the desired flow direction into the next blade row is not achieved. In predicting the performance of a turbomachine at operating points other than design, it is necessary to estimate the direction of the flow leaving blades of specified geometry. Incorrect estimation of these flow angles will lead to faulty prediction of energy transfer in rotors and incorrect values of estimated loss in subsequent blade rows. Thus, estimating leaving flow angles is a critical part of both design and analysis calculations.

Historically, for many compressor applications, the direction of the flow leaving a blade cascade has been predicted by estimating the difference between the average direction of the leaving flow and the direction of the blade mean line at the trailing edge. This difference is defined as deviation angle. Measurements indicate that generally the flow is not turned far enough to leave the blade row in the direction of the blade mean line. This happens because inertia resists the forces exerted on the fluid to produce turning. The forces which produce turning in a cascade result from the curvature of the blade passage. However, blade passages tend to be too short to guide the fluid perfectly.

No completely satisfactory methods for estimating deviation angle are available even for the simpler case of design-point operation (ref. 1). The last major improvement in deviation-angle estimation methods was published in 1946 (ref. 2). In the past the search for better deviation-angle prediction methods was restricted mainly to correlations of experimental data. Theoretical calculations of both potential flow and boundary-layer flow were possible but not widely used. Conformal transformation calculations of potential flow, for example, were too time consuming to be practical. Boundary-layer calculations were not practical on a large scale either, if for no other reason than because they required surface pressure distributions from a potential-flow solution as input. However, recent advances in the size and speed of digital computers have made it practical to obtain large numbers of theoretical solutions for some two-dimensional flows. These analytical procedures are increasingly being used to supplement, and in some cases to supplant, experimental studies.

The purpose of this report is to begin development of a more satisfactory method of estimating deviation angle by applying currently available analytical procedures to the problem. A flow model was chosen for the study which was simple enough to treat theoretically while still close enough to real flows to allow useful results to be obtained. Simplifications to the real flow included the assumptions that flow was steady and two dimensional. While viscous effects were recognized as important, they were omitted in

this work, although suggestions for future inclusion are given. Deviation angles estimated for a plane cascade by using an existing inviscid-flow computer program were compared with experimental data.

MODELING TURBOMACHINERY FLOW

In this section the need for simplifying assumptions in treating turbomachinery flow is indicated. It is obviously important to use consistent flow models in both experimental and theoretical work so that valid comparisons of results can be made. A widely used flow model which was chosen for this study is described. Symbols used throughout are defined in the appendix.

Experimental Cascade Models

Annular-cascade models. - The real flow in a compressor is three dimensional, unsteady, turbulent, and compressible, with significant viscous forces in portions of the flow region. In addition, the flow is bounded by both moving and stationary walls which are highly complicated in shape. It is not yet possible to obtain a solution of this difficult fluid mechanics problem either theoretically or experimentally without introducing simplifying assumptions. The most common flow model used assumes the flow to be represented by steady, circumferentially averaged[†] velocities, angles, and fluid properties at a discrete number of stations, as indicated in figure 1. These stations are often, though not always, located in r-θ planes which are outside the blade rows. The flow is assumed to be steady relative to each blade row although in a real machine this is impossible except for the first blade row. Viscous effects are neglected locally, but the accumulated viscous effects in the form of total-pressure losses along a stream surface are included. Stream surfaces are assumed to be surfaces of revolution, as illustrated in figure 2. This sketch is an approximation since the real stream surfaces are probably skewed and warped near the blades and are even more complicated in shape near the annulus walls. Circumferentially averaged velocities, angles, and fluid properties are defined on these surfaces to represent the flow at a given radius and axial location.

[†]Ideally, mass-weighted circumferential averages are used. However, in practice, several kinds of averages are substituted for a true mass-weighted circumferential average. At stations behind rotating blades, time-averaged velocities, angles, pressures, and temperatures measured with low-frequency-response probes at fixed circumferential locations are often used. Data from circumferential traverses or from rakes are frequently area weighted to define averages behind stationary blade rows.

When the stream surface of revolution is assumed to be a right-circular cylinder, it can be developed to show the intersections of the blades, as illustrated in figure 3. The circumferentially averaged velocity at the trailing edge of the blades is represented by the vector W_2. The associated flow angle referenced to the axial direction is β_2'. Deviation angle δ is defined as the angle between the W_2 vector and the tangent to the blade mean line at the trailing edge (see fig. 3). A more general stream surface of revolution (i.e., other than a cone) cannot be developed into an undistorted plane. In this case the exit blade angle κ_2 and the velocity W_2 are ordinarily defined on the plane tangent to the stream surface at the trailing edge. Deviation angle is then defined in the same plane.

Ultimately, the deviation-angle distribution for an annular cascade, rotating or stationary, is determined (for a given fluid and given inlet flow conditions and rotational speed) by the geometric shape and arrangement of the blades and the annulus boundaries. Thus, to estimate deviation angle for one stream surface in the flow model described, it is necessary to consider not only the blade geometry of that surface, but also the blade geometry of all other stream surfaces and the annulus wall shapes. In addition, fluid properties, inlet flow conditions, and rotational speed must be considered. The number of geometric variables alone indicates the difficulty of developing a general deviation-angle prediction method by correlating experimental data.

A further simplification of the flow model is necessary in order to estimate deviation angles for each stream surface. The usual approach is to assume that the local blade geometry (i.e., blade geometry on the stream surface) has the dominant effect on deviation angle. The influences of the remaining flow boundaries, the inlet flow conditions, and the rotational speed are accounted for by correction factors based on tests of similar blade rows or by testing and redesigning.

Plane-cascade models. - The influence of the local blade geometry on deviation angle can be studied by using the untwisted blades of a plane, two-dimensional cascade. Two-dimensional flow is assured by using the same blade section along the entire blade span and by removing boundary-layer fluid from the tunnel walls. Plane-cascade flow is obviously simpler than flow in actual machines. For example, spanwise gradients of flow parameters are absent, as are annulus boundary layers, tip clearance flows, and centripetal forces. Although a real, viscous fluid is used, blade surface boundary layers are two dimensional rather than three dimensional. These simplifications in the flow model provide a significant advantage because tests can be made in which the blade-section geometric parameters are varied systematically one at a time. This is not possible in annular cascades. Systematic testing has been reported for a few blade profile families (e.g., refs. 3 to 8), but the number of variables involved makes exhaustive testing impractical. Thus, many combinations of geometric parameters are encountered for which extrapolation of test data is required. Extrapolation is always undesirable because of the added uncertainty it introduces. Furthermore, empirical correlations based on

plane-cascade data tend to lack generality with respect to blade profile shape (thickness distribution and mean-line shape).

The problems of extrapolation and restriction to particular blade profiles associated with the use of correlated plane-cascade data can be avoided by calculating the flow in the blade-to-blade plane analytically. In view of the seemingly advanced state of the art of calculations of flow about airfoils, it seems that using a theoretical model would be feasible.

Theoretical Cascade Model

An exact theoretical calculation of plane, two-dimensional cascade flow that accounts for the unsteadiness implicit in real turbulent flow and that is capable of describing regions of separated flow is currently impossible. Consequently, we must use simplified flow models which retain enough features of real flow to yield useful results. A well-developed approach is to divide the flow field into two parts, with viscous boundary-layer flow in a thin region near the blade surface and inviscid irrotational flow in the remainder of the field. For flows with high Reynolds number and little or no separation, useful results can often be obtained by assuming inviscid flow throughout the cascade flow field.

A number of methods have been developed and published for calculating flow through a plane cascade by using an inviscid-flow model. Reviews of typical methods are given by Roudebush (ref. 9), Scholz (ref. 10), and Schilhansl (ref. 11). The inviscid-flow models used have many features in common. The flow field typically contains a single row of blades with uniform flow assumed at some distance upstream and downstream from the blades. The flow is assumed to be steady, inviscid, and irrotational; but it is not always assumed to be incompressible. These assumptions can be combined with the continuity and momentum equations to define a governing partial differential equation for the stream function or velocity potential throughout the flow field.

Boundary conditions must be given to complete the statement of the mathematical problem for subsonic flow. One condition required is that the blade profile form a streamline in the flow. Additional conditions must be given which determine the location of the stagnation points near the leading and trailing edges. The leading-edge stagnation point can be readily located by specifying the direction of the upstream uniform flow since this is usually given or known in advance. The location of the trailing-edge stagnation point, or equivalently the direction of the uniform downstream flow, also must be given to complete the mathematical statement of the flow problem.

In real flow, viscous forces play a key role in determining the blade circulation or, equivalently, the leaving flow angle. But the inviscid-flow problem is still indeterminate unless the leaving flow angle or the trailing-edge stagnation point is specified. There is

a different mathematically complete inviscid-flow solution for each of the infinite number of locations which can be specified for the trailing-edge stagnation point. Since the objective is to obtain a theoretical flow solution which approximates the real flow as closely as possible, the choice of the rear stagnation point location must be based on some knowledge of real flow patterns.

In the somewhat academic case of blades with either sharp or cusped trailing edges, the Kutta condition (ref. 12) is used as the trailing-edge condition. The Kutta condition requires that the velocities on the pressure and suction surfaces be equal at the trailing-edge point. Equality of velocity implies a stagnation point if the blade surfaces form a wedge at the trailing edge, but not if they form a cusp. Imposing the Kutta condition on the problem avoids the physically implausible condition of an infinite velocity at a sharp trailing edge. Unfortunately, the Kutta condition does not apply to blades with rounded trailing edges, which are normally used in turbomachines to lower material stresses. No generally accepted trailing-edge hypothesis analogous to the Kutta condition exists for rounded-trailing-edge blades, although several proposals have been advanced. Three of these proposed trailing-edge hypotheses (refs. 13 to 15) are evaluated in the section DEVIATION-ANGLE ESTIMATION.

Solutions of the completely specified inviscid-cascade-flow problem can be obtained by a number of mathematical techniques. For incompressible flow the governing equation is Laplace's equation, which can be solved by conformal transformation, by superposition of singularities on a uniform flow, or by a numerical finite-difference technique. Conformal transformation methods remain relatively slow and are not widely used (ref. 10). Singularity techniques have been published by Schlichting (ref. 16), Martensen (ref. 17), and Giesing (ref. 18), among others. Katsanis (ref. 19) has published a computer program which uses a numerical finite-difference technique to solve for the incompressible flow in cascades.

For compressible flow, the partial differential equations for stream function and velocity potential have the form of Poisson's equation. They have been solved for subsonic compressible flow by Imbach (ref. 20), who used a singularity solution, and by Katsanis (ref. 21) and Smith (ref. 22), who used finite-difference techniques.

The computer program by Katsanis (ref. 21) was chosen for use in this study. The reasons for its choice include its capability of handling both compressible and incompressible flow and the availability of an auxiliary program (ref. 23) which allows finer definition of flow details near the trailing edge.

INVISCID-FLOW COMPUTER PROGRAMS

Only a brief description of the inviscid-flow computer programs is given here. For more details, references 21 and 23 should be consulted. The programs TSONIC (ref. 21)

and MAGNFY (ref. 23) are basically similar; and the description applies to both, with the few differences noted appropriately. The programs were written in a general form, which permits calculation of flow on a surface of revolution for an annular cascade, either rotating or stationary, as well as for the simpler case of a plane cascade. The surface of revolution is assumed to be a stream surface. The calculation region for the general case is shown in figure 4. The (r, θ, z) coordinates of the surface were mapped into a (m, θ) plane by functional relations

$$\theta = \theta$$

$$m = m(r, z)$$

The resulting calculation regions in the $m\text{-}\theta$ plane are shown in figure 5.

The flow on the assumed stream surface in figure 4 is further simplified from the real flow by the following assumptions:

(1) The flow is steady relative to the blades.

(2) The fluid is an ideal gas with constant c_p or is incompressible.

(3) The fluid is nonviscous, and there is no heat transfer. (Therefore, the flow is isentropic.)

(4) The stagnation temperature and the velocity vector are uniform across the inlet boundary. (Therefore, the flow is irrotational in absolute coordinates as well as isentropic.)

(5) The velocity is uniform across the downstream boundary.

(6) The only forces are those resulting from the momentum and pressure gradient.

(7) The flow is subsonic, except that TSONIC allows small areas of low supersonic flow.

In this study the full capabilities of the TSONIC program were not required since only low subsonic flow in plane cascades was computed. Therefore, the transonic-flow calculation subroutines were removed from TSONIC, essentially reducing it to the subsonic TURBLE program reported in reference 24.

The preceding assumptions were incorporated into the continuity equation and the equation of motion, which were then combined into a second-order partial differential equation for the stream function. The derivation is presented in reference 25. The equation for the stream function u used in TSONIC and MAGNFY can be obtained from equation 12(9) of reference 25 by substituting $-uw$ for the stream function of reference 25. The resulting equation is

$$\frac{1}{r^2}\frac{\partial^2 u}{\partial \theta^2} + \frac{\partial^2 u}{\partial m^2} - \frac{1}{r^2}\frac{1}{\rho}\frac{\partial \rho}{\partial \theta}\frac{\partial u}{\partial \theta} + \left[\frac{\sin \alpha}{r} - \frac{1}{b\rho}\frac{\partial (b\rho)}{\partial m}\right]\frac{\partial u}{\partial m} = \frac{2b\rho\omega}{w}\sin \alpha \qquad (1)$$

The stream function u is normalized by the mass flow per blade channel w so that it has a value of 0 on surface BC of figure 5 and 1 on surface GF. The stream function is related to velocity by the equations

$$\frac{\partial u}{\partial m} = -\frac{b\rho}{w} W_\theta \tag{2}$$

$$\frac{\partial u}{\partial \theta} = \frac{b\rho r}{w} W_m \tag{3}$$

Equation (1) is elliptic, and boundary conditions must be specified for the solution regions of figure 5. Along BC and FG (fig. 5) the stream function is assigned values of 0 and 1 as previously stated. The assumed periodicity of the flow in the θ-direction allows the stream function on HG to be specified as the stream-function value on AB for the same m-value plus 1. The same kind of periodic boundary condition is applied to lines CD and EF in figure 5. Along AH and DE, $\partial u/\partial m$ is specified. Evaluation of $\partial u/\partial m$ on AH is possible since a uniform flow is assumed. Thus, by equation (2)

$$\left(\frac{\partial u}{\partial m}\right)_{AH} = \left(-\frac{b\rho}{w} W_\theta\right)_{AH} = \left(-\frac{b\rho}{w} W_m \tan \beta_1'\right)_{AH} = \left(-\frac{1}{r}\frac{\partial u}{\partial \theta} \tan \beta_1'\right)_{AH} \tag{4}$$

But the flow is uniform and periodic along AH; so

$$\frac{1}{r}\left(\frac{\partial u}{\partial \theta}\right)_{AH} = \frac{u(H) - u(A)}{r[\theta(H) - \theta(A)]} = \frac{1}{s} \tag{5}$$

Substituting equation (5) into equation (4)

$$\left(\frac{\partial u}{\partial m}\right)_{AH} = -\frac{1}{s_{AH}} \tan \beta_1' \tag{6}$$

Similarly, it can be shown that

$$\left(\frac{\partial u}{\partial m}\right)_{DE} = -\frac{1}{s_{DE}} \tan \beta_2' \tag{7}$$

The angles β_1' and β_2' must be obtained from input information.

Boundary conditions for MAGNFY are set by specifying the value of the stream function on all segments of the boundary (fig. 5). Stream-function values from TSONIC output

are specified at discrete points on OPQRST. The stream function is set to zero on the blade surface ST.

For this study, both TSONIC and MAGNFY were modified to provide blade surface pressure coefficients at the intersections of the mesh lines and blade surfaces as additional output. The points of intersection were assigned a fraction of chord value by projecting each point onto the chord line (fig. 5) and dividing the length x by the length of the chord line. The coding changes and additions necessary to generate this additional output are given in reference 26.

The programs were run on an IBM 7094-2/7044 direct-coupled system.

DEVIATION-ANGLE ESTIMATION

Deviation angles and blade surface pressure distributions calculated for a zero-thickness flat-plate cascade and a thick cambered cascade are presented in this section. As noted in the section Theoretical Cascade Model, estimating deviation angle by using an inviscid-flow calculation requires some assumption regarding the flow around the trailing edge. The Kutta condition was used in the flat-plate calculations, and the results were compared with the conformal mapping theory of Weinig (ref. 27). Results for the cambered cascade were calculated with three different trailing-edge hypotheses and are compared with experimental data.

Flat-Plate Calculation

A numerical solution for the flow through a flat-plate cascade satisfying the Kutta condition was calculated by using the TSONIC program. Calculations were made for a cascade with a 20° blade setting angle, a solidity of 1.0, and a 30° inlet flow angle. Pressure distributions and stagnation streamlines which correspond to zero circulation (for reference) and to the circulation fixed by the Kutta condition are shown in figures 6 to 8. The deviation angle for which the dividing streamline leaves the blade at the trailing-edge point (Kutta condition) was found to be 0.48° (fig. 8). A deviation angle of 0.48° was also calculated for the same cascade by using the conformal mapping results of Weinig (ref. 27). The excellent agreement between the two methods is a basis for confidence in the numerical techniques used in the TSONIC and MAGNFY programs and in the stagnation streamline extrapolation procedure used to locate the rear stagnation point. The dividing streamlines were extrapolated from the vertical mesh line nearest to the blade by using a computer program (STGPLS) described in reference 26.

Selection of Cambered Airfoil Cascade

Several features were required in the cambered airfoil section chosen to evaluate deviation-angle estimation by using the inviscid-flow computer programs. The first requirement was availability of reliable plane-cascade air data with a systematic variation of incidence angle and inlet flow angle. Plane-cascade flow was the most logical choice to compare with the calculated flow because it is the real flow most closely approximated by the mathematical model used. The section was required to have a well-defined rounded trailing edge. This requirement eliminated the NACA 65-series profile. Also a section with a camber angle low enough to avoid extensive regions of flow separation except at high incidence angles was desired. All these requirements were satisfied by the 10C4/30C50 blade section. A systematic set of plane-cascade measurements for this blade are given in reference 28. An additional advantage of these data was that the tests were carefully conducted to produce two-dimensional flow conditions. Coordinates describing the 10C4/30C50 section given in reference 28 were used to generate geometric input for the inviscid-flow solutions presented in the remainder of this section. The flow and blade angles for which deviation angles were estimated are summarized in table I.

Calculations Using Experimental Deviation Angles

It is of considerable interest to compare the inviscid-flow solutions calculated by using the experimentally determined deviation angles for a decelerating cascade with measurements of the real flow. The features of most interest in the inviscid solutions are (1) the blade surface pressure distributions because of their strong influence on boundary-layer development and the resulting losses and (2) the stagnation streamlines because of the dependence of deviation angle on the location of the rear stagnation point. Calculated and measured pressure distributions for the 10C4/30C50 profile in cascade are compared in figures 9 and 10. These comparisons are generally good, with the largest discrepancies occurring near the leading edge. Pressure measurements over the last 30 percent of chord were not given in reference 28 for most operating points, and thus are not shown except in figure 9(b).

A typical stagnation streamline calculated by using the experimental deviation angle is shown in figure 11 for a 10C4/30C50 cascade with inlet flow angle of 30°. The stagnation streamline for zero circulation is shown for reference.

Calculations Using Three Trailing-Edge Hypotheses

Wilkinson's hypothesis. - Wilkinson (ref. 14) suggests that the simplest form of trailing-edge hypothesis is to locate the rear stagnation point at the point of maximum curvature or at the end of the mean camber line. The circular trailing edge of a 10C4/30C50 has no single point of maximum curvature, so the stagnation point was located at the end of the mean camber line for this study. A series of calculations were required to determine the outlet flow angle (used as a boundary condition in TSONIC) for which the rear stagnation point coincided with the end of the mean camber line. Pressure distributions (fig. 12) and stagnation streamlines were obtained for several values of deviation angle (fig. 13). The resulting relation between deviation angle and stagnation point location (fig. 14) was interpolated to obtain the deviation angle for which the stagnation point fell on the end of the mean camber line. The deviation angles so obtained are compared with measured values in figure 15(a). The estimated deviation angles shown in figure 15(a) are from 2.6° to 6.4° lower than the measured angles.

Closure hypothesis. - Another trailing-edge hypothesis commonly used (ref. 15) is to set the leaving angle so that the curves of pressure or velocity for the two surfaces cross at the trailing edge ($x/c = 1.0$). This necessarily requires an extrapolation of the calculated curves (fig. 16) since the inviscid-flow velocities on one or both surfaces often exhibit rapid accelerations near the trailing edge before rapidly decelerating to reach the stagnation point. The changes in surface pressure at the trailing edge probably do not occur as rapidly in real flow because of the presence of the surface boundary layers and the wake. Thus, the local acceleration on the suction surface in figure 16 beginning at an x/c of 0.95 was ignored in applying the closure hypothesis. Justification for applying this trailing-edge hypothesis is the supposition that in real flow the surface pressures approach a common value which exists in the wake in the immediate vicinity of the trailing-edge circle. Furthermore, the surface pressure distribution near and on the trailing edge from the inviscid solution is not likely to bear much resemblance to the real pressure distribution as previously explained. Thus, extrapolating the surface pressure curves from a point away from the trailing edge is an effort to obtain a better approximation to the pressure distribution of real flow than that obtainable from inviscid-flow calculations. The assumption is that a continuation of the inviscid pressure curves toward the trailing edge is a good approximation of the real pressure distribution. There are difficulties inherent in the method, including determination of the point where the extrapolation should begin and the shapes of the extrapolated curves. In this study, graphical extrapolations of the suction- and pressure-surface pressure distributions were started at x/c of 0.94 and 0.97, respectively. The shapes of the extrapolated curves were constructed by using a drafting curve to be a continuation of the shape of the calculated curves at those points.

Estimating deviation angle by using this hypothesis is a trial-and-error process. Pressure distributions calculated for several values of deviation angle are extrapolated until the curves for the two surfaces cross or close. The x/c value where the curves cross is plotted as a function of δ, and the resulting curve is interpolated at an x/c of 1.0 to obtain the estimated deviation angle δ_c. The curves of δ as a function of $(x/c)_{cl}$ for the C4 cascade at inlet flow angles of 30° and 60° are shown in figures 17 and 18. For every 1 percent change in $(x/c)_{cl}$ the corresponding deviation-angle change is 0.5° to 0.7°. The estimated deviation angles δ_c are compared with the measured values in figure 15. In general, the deviation angles estimated by using this hypothesis are significantly lower than the measured angles.

The pressure distributions calculated by using the estimated deviation angles are shown in figures 19 and 20. Measured pressures are shown for comparison. The discrepancies between measured and calculated pressure coefficients in figures 19 and 20 are approximately the same or generally slightly larger than those which resulted when experimental deviation angles were used in the calculation (figs. 9 and 10).

Gostelow's hypothesis. - Gostelow, Lewkowicz, and Shaalan (ref. 13) suggest that an appropriate approach is to linearly extrapolate the surface pressure curves from $x/c = 0.85$ until they cross. The correct deviation angle is assumed to be the value for which the extrapolated curves cross at $x/c = 1.0$. An example pressure distribution showing how the curves are extrapolated is shown in figure 21. To estimate deviation angle with this hypothesis, a series of calculations are made for different deviation angles; and plots similar to figure 21 are constructed. Then a plot of δ against $(x/c)_{int}$ is extrapolated to obtain the δ which corresponds to an $(x/c)_{int}$ of 1.0.

Deviation angles were estimated for the 10C4/30C50 cascade over a range of incidence angles at inlet flow angles of 30° and 60°. The curves of δ against $(x/c)_G$ are shown in figures 22 and 23. The estimated deviation angles δ_G are compared with measured values in figure 15. The calculated deviation angles are reasonably close to the measured angles except at high incidence angles, where increased drag coefficients (ref. 28) indicate thickened and possibly separated suction-surface boundary layers. Calculated and measured pressure distributions are compared in figures 24 and 25. Discrepancies between the calculations and measurements shown in figures 24 and 25 are slightly greater than those in figures 9 and 10.

Variable-closure hypothesis. - A new trailing-edge hypothesis is proposed based on calculations made in this study. In examining pressure distributions calculated with experimental deviation angles, it was observed that the pressure curves all crossed at $x/c < 1.0$ (figs. 9 and 10). Furthermore, the percent chord location at which the curves crossed decreased as incidence angle increased at a given inlet flow angle.

The variable-closure hypothesis was developed on the basis of these observations and the following reasoning: As incidence angle varies, the change in measured deviation

angle, and thus the change in the location at which the corresponding inviscid-flow pressure distribution crosses, is probably closely related to the thickness of the boundary layer on the suction surface. The boundary-layer thickness is, in turn, dependent on the velocity deceleration which takes place on the suction surface. Thus, the pressure-distribution crossing location calculated with the experimental deviation angle should be related to the decrease in pressure coefficient on the suction surface. In figure 26 the chordwise location where the inviscid pressure distributions calculated with experimental deviation angles cross is shown as a function of the pressure coefficient change on the suction surface. The pressure coefficient change used was the difference between the maximum pressure coefficient at x/c, where $0.05 \leq x/c \leq (x/c)_{cl}$, and the pressure coefficient at $(x/c)_{cl}$. The calculated curves in figures 9 and 10 were used to obtain the points plotted in figure 26. No claims can be made for the generality of the relation shown in figure 26 except that it holds over a fairly wide range of incidence angle and blade setting angle for the 10C4/30C50 section.

DISCUSSION OF RESULTS

Of the three existing trailing-edge hypotheses used to estimate deviation angle, Gostelow's was most successful (fig. 15). It resulted in rather close estimation (within 1°) of deviation angle over a substantial range of incidence angles at blade setting angles of 30° and 60°. However, at high incidence angles, where reference 28 indicates that the coefficient of drag was approximately twice the minimum value, the deviation angles estimated by using Gostelow's method are significantly lower than the measurements. This indicates that the method cannot be expected to work well for highly loaded blades with significant areas of separated flow.

Wilkinson's hypothesis underestimated deviation angles by a significant fraction of the total turning. Such an arbitrary location for the rear stagnation point would give good results only if a small change in deviation angle corresponded to a rather large shift in stagnation point location. However, as indicated in figures 11 and 13, the opposite is true, so the stagnation point must be located quite exactly to estimate deviation angle accurately.

The closure hypothesis resulted in significant underestimation of deviation angles over the entire operating range (fig. 15). In fact, as previously noted, the pressure distribution curves calculated with experimental deviation angles all crossed at $x/c < 1.0$ (figs. 9 and 10).

REMARKS

The general lack of agreement between estimated and measured deviation angles at high incidence angles (fig. 15) suggests that viscous effects must be included in any general deviation-angle estimation procedure. One simplified approach is to use the proposed variable-closure trailing-edge hypothesis based on figure 26 in which the closure location is a function of the inviscid-flow suction-surface pressure distribution. This hypothesis should be evaluated for a range of profile shapes, camber angles, solidities, inlet Mach numbers, and axial velocity ratios.

A better general approach would incorporate viscous flow calculations directly into the deviation-angle estimation method. This could be done in principle by calculating the inviscid and boundary-layer flow and applying Preston's theorem (ref. 29) to the combined flow solution. Preston's theorem, for the case of an airfoil with steady, irrotational, approaching flow, asserts that the net vorticity shed from the blade surface boundary layers into the wake must be zero. This idea has been applied to isolated airfoils (ref. 29) but so far has not been fully evaluated for cascade flow (ref. 13). Several difficulties would be encountered in calculating the required boundary layers for cascades. These include accurate prediction of transition, calculation of turbulent boundary layers in large adverse pressure gradients, prediction and description of the separated flow, and inclusion of wake properties. However, the fundamental nature of this approach warrants a careful evaluation to assess whether viscous flow theory is mature enough to be incorporated into a deviation-angle estimation method.

CONCLUSIONS

Development of a more satisfactory procedure of estimating deviation angles over a range of incidence angles by using inviscid-flow calculations was begun. Since the outlet flow angle is required to solve the inviscid-flow equations, a trial-and-error procedure involving a trailing-edge hypothesis was required to estimate deviation angle. The trailing-edge hypothesis suggested by Gostelow was found to give satisfactory results except at high incidence angles. Locating the rear stagnation point at the end of the mean camber line was found to be unsatisfactory as a trailing-edge hypothesis. Requiring a curved extrapolation of the pressure distributions to close at the trailing edge also proved to be an unsatisfactory procedure. A new trailing-edge hypothesis applicable to

the 10C4/30C50 blade section over a wide range of incidence and blade setting angles is presented.

Lewis Research Center,
National Aeronautics and Space Administration,
Cleveland, Ohio, November 20, 1973,
501-24.

APPENDIX - SYMBOLS

b	stream tube thickness, m
C_{p_i}	pressure coefficient, $(P_1^o - p_l)/\frac{1}{2}\rho_1 V_1^2$
c	blade chord (fig. 3), m
c_p	specific heat at constant pressure, J/kg-K
i	incidence angle (fig. 3), deg
M	Mach number
m	meridional coordinate (fig. 4), deg
P^o	stagnation pressure in absolute coordinate system, N/m^2
p	static pressure, N/m^2
r	radius from axis of rotation (fig. 4), m
s	blade spacing (fig. 3), m
u	stream function (eqs. (2) and (3))
V	fluid absolute velocity, m/sec
W	fluid velocity relative to blade, m/sec
w	mass flow in stream tube between two blades, kg/sec
x	distance along chord from leading edge, m
x/c	fraction of chord
z	axial coordinate (fig. 4), m
α	angle between tangent to stream surface and axial direction (fig. 1), deg
β	angle between flow direction and axial direction (fig. 3), deg
Γ	blade circulation, $s(V_{\theta,1} - V_{\theta,2})$, m^2/sec
γ	blade setting angle (fig. 3), deg
δ	deviation angle, angle between relative velocity and tangent to mean camber line at trailing edge (fig. 3), deg
θ	angular coordinate (fig. 4), rad
κ	blade angle, angle between tangent to mean camber line and axial direction (fig. 3), deg
ξ	angular distance on trailing-edge circle between axial direction and stagnation point (fig. 17), deg

ρ fluid density, kg/m^2

σ blade solidity, defined as c/s

ω rotational speed, rad/sec

Subscripts:

AH along line AH in fig. 5

c obtained with closure trailing-edge hypothesis

cl where pressure coefficient curves close or cross

DE along line DE in fig. 5

exp experimental value

G obtained with Gostelow's trailing-edge hypothesis

int where linearly extrapolated pressure coefficient curves intersect

l local value on blade surface

m meridional component

max maximum

W obtained with Wilkinson's trailing-edge hypothesis

θ tangential component

1 blade row entrance

2 blade row exit

Superscript:

' relative to blade

REFERENCES

1. Miller, Max J.: Deviation Angle Prediction Methods - A Review. Rep. ERI-580, Iowa State Univ. (NASA CR-106959), Oct. 1969.

2. Carter, A. D. S.; and Hughes, Hazel P.: A Theoretical Investigation Into the Effect of Profile Shape on the Performance of Aerofoils in Cascade. Rep. R&M-2384, Aeronautical Research Council, Gt. Britain, Mar. 1946.

3. Emery, James C.; Herrig, L. Joseph; Erwin, John R.; and Felix, A. Richard: Systematic Two-Dimensional Cascade Tests of NACA 65-Series Compressor Blades at Low Speeds. NACA Rep. 1368, 1958.

4. Matsuki, Masakatsu; and Takahara, Kitao: Cascade Tests of High Stagger Compressor Blades. Japan Soc. Mech. Eng. Bull., vol. 5, no. 18, 1962, pp. 277-291.

5. Taylor, W. E.; Murrin, T. A.; and Colombo, R. M.: Systematic Two-Dimensional Cascade Tests. Vol. 1: Double Circular-Arc Hydrofoils. Rep. UARL-H910254-50, United Aircraft Corp. (NASA CR-72498), Dec. 19, 1969.

6. Taylor, W. E.; Murrin, T. A.; and Colombo, R. M.: Systematic Two-Dimensional Cascade Tests. Vol. 2: Multiple Circular-Arc Hydrofoils. Rep. UARL-J910254-56, United Aircraft Corp. (NASA CR-72499), Apr. 6, 1970.

7. Colombo, R. M.; and Murrin, T. A.: Systematic Two-Dimensional Cascade Tests. Vol. 3: Slotted Double Circular-Arc Hydrofoils. Rep. UARL-L930845-81, United Aircraft Corp. (NASA CR-72870), May 1, 1972.

8. Ikui, T.; Inoue, M.; and Kaneko, K.: Two-Dimensional Cascade Performance of Circular-Arc Blades. Tokyo Joint International Gas Turbine Conference and Products Show Proceedings. Japan Soc. Mech. Eng., 1971, pp. 57-64.

9. Roudebush, William H.: Potential Flow in Two-Dimensional Cascades. Aerodynamic Design of Axial-Flow Compressors. Irving A. Johnsen and Robert O. Bullock, eds. NASA SP-36, 1965, pp. 101-149.

10. Scholz, N.: A Survey of the Advances in the Treatment of the Flow in Cascades. International Aerodynamics (Turbomachinery). Inst. Mech. Eng., 1970, pp. 20-31.

11. Schilhansl, Max J.: Survey of Information on Two-Dimensional Cascades. Brown Univ. (WADC-TR-54-322), Mar. 1955.

12. Landau, L. D.; and Lifshitz, E. M.: Fluid Mechanics. Addison-Wesley Publ. Co., Inc., 1959.

13. Gostelow, J. P.; Lewkowicz, A. K.; and Shaalan, M. R. A.: Viscosity Effects on the Two-Dimensional Flow in Cascades. Rep. ARC-CP-872, Aeronautical Research Council, Gt. Britain, 1967.

14. Wilkinson, D. H.: Discussion. Thermodynamics and Fluid Mechanics. Vol. 2: Axial and Radial Turbomachinery. Proc. Inst. Mech. Eng., vol. 184, pt. 3G(II), 1970, pp. 113-116.

15. Sanger, Nelson L.: Analytical Study of the Effects of Geometric Changes on the Flow Characteristics of Tandem-Bladed Compressor Stators. NASA TN D-6264, 1971.

16. Schlichting, Hermann: Berechung der reibungslosen inkompressiblen Strömung für ein vorgegebenes ebenes Schaufelgitter. VDI Forschungheft, no. 447, 1955.

17. Martensen, E.: The Calculation of the Pressure Distribution on a Cascade of Thick Airfoils by Means of Fredholm Integral Equations of the Second Kind. NASA TT F-702, 1971.

18. Giesing, Joseph P.: Extension of the Douglas Neumann Program to Problems of Lifting, Infinite Cascades. Rep. LB-31653, Douglas Aircraft Co., Inc., (AD-605207), July 2, 1964.

19. Katsanis, Theodore: A Computer Program for Calculating Velocities and Streamlines for Two-Dimensional, Incompressible Flow in Axial Blade Rows. NASA TN D-3762, 1967.

20. Imbach, H. E.: Calculation of the Compressible, Frictionless Subsonic Flow Through a Plane Blade Cascade. Brown Boveri Rev., vol. 51, no. 12, Dec. 1964, pp. 752-761.

21. Katsanis, Theodore: FORTRAN Program for Calculating Transonic Velocities on a Blade-to-Blade Stream Surface of a Turbomachine. NASA TN D-5427, 1969.

22. Smith, D. J. L.: Computer Solutions of Wu's Equations for the Compressible Flow Through Turbomachines. Fluid Mechanics and Design of Turbomachinery. B. Laksminarayana, W. R. Britsch, and W. S. Gearhart, eds. NASA SP-304, 1973, pp. 60-114.

23. Katsanis, Theodore; and McNally, William D.: FORTRAN Program for Calculating Velocities in a Magnified Region on a Blade-to-Blade Stream Surface of a Turbomachine. NASA TN D-5091, 1969.

24. Katsanis, Theodore: Computer Program for Calculating Velocities and Streamlines on a Blade-to-Blade Stream Surface of a Turbomachine. NASA TN D-4525, 1968.

25. Vavra, Michael H.: Aero-Thermodynamics and Flow in Turbomachines. John Wiley & Sons, Inc., 1960.

26. Miller, Max J.: Some Aspects of Deviation Angle Estimation for Axial-Flow Compressors. Ph.D. Thesis, Iowa State Univ., 1973.

27. Weinig, Fritz: Die Strömung um die Schaufeln von Turbomaschinen. Johann Ambrosius Barth, Leipzig, 1935.

28. Felix, A. Richard; and Emery, James C.: A Comparison of Typical National Gas Turbine Establishment and NACA Axial-Flow Compressor Blade Sections in Cascade at Low Speeds. NACA TN 3937, 1957.

29. Preston, J. H.: The Calculation of Lift Taking Account of the Boundary Layer. Rep. R&M-2725, Aeronautical Research Council, Gt. Britain, 1953.

TABLE I. - CASCADE CONDITIONS FOR WHICH DEVIATION ANGLES WERE ESTIMATED

[10C4/30C50 profile; blade solidity, σ, 1.0; Mach number at blade row entrance, M_1, 0.08.]

Inlet flow angle, β_1, deg	Incidence angle, i, deg	Experimental deviation angle, δ_{exp}, deg	Blade setting angle, γ, deg
30	-7.7	8.8	22.7
	.3	8.7	14.7
	11.3	12.15	3.7
60	-9.0	10.45	54.0
	-1.2	11.3	46.2
	6.6	14.4	38.4

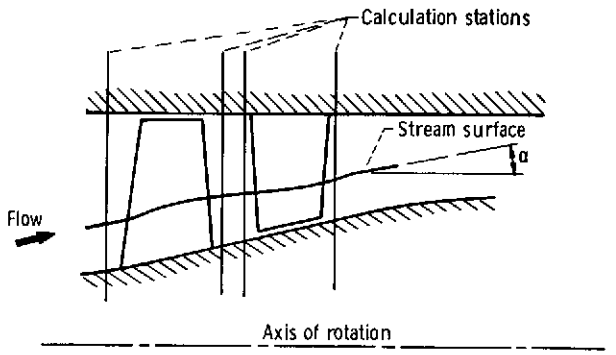

Figure 1. - Meridional plane cross section of an axial-flow compressor stage.

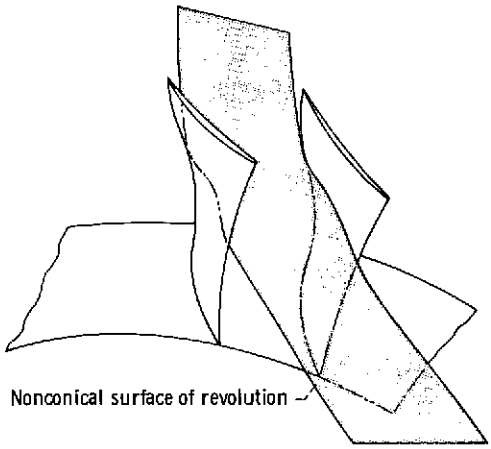

Figure 2. - Sketch of a general stream surface of revolution.

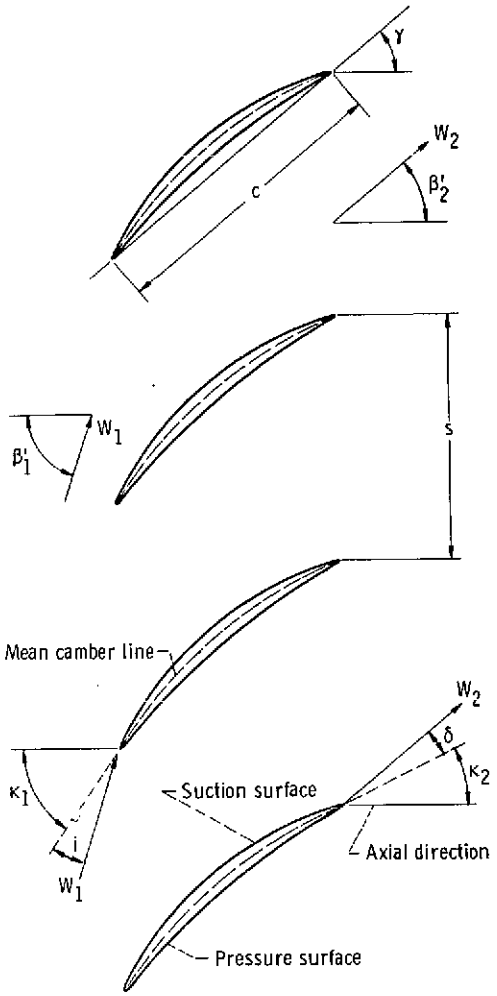

Figure 3. - Cascade view of blade sections and blade nomenclature.

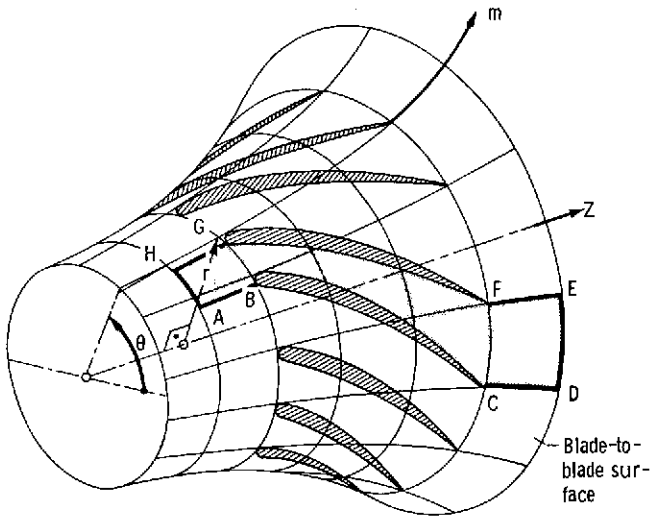

Figure 4. - Blade-to-blade surface of revolution, showing m-θ coordinates. (From ref. 21.)

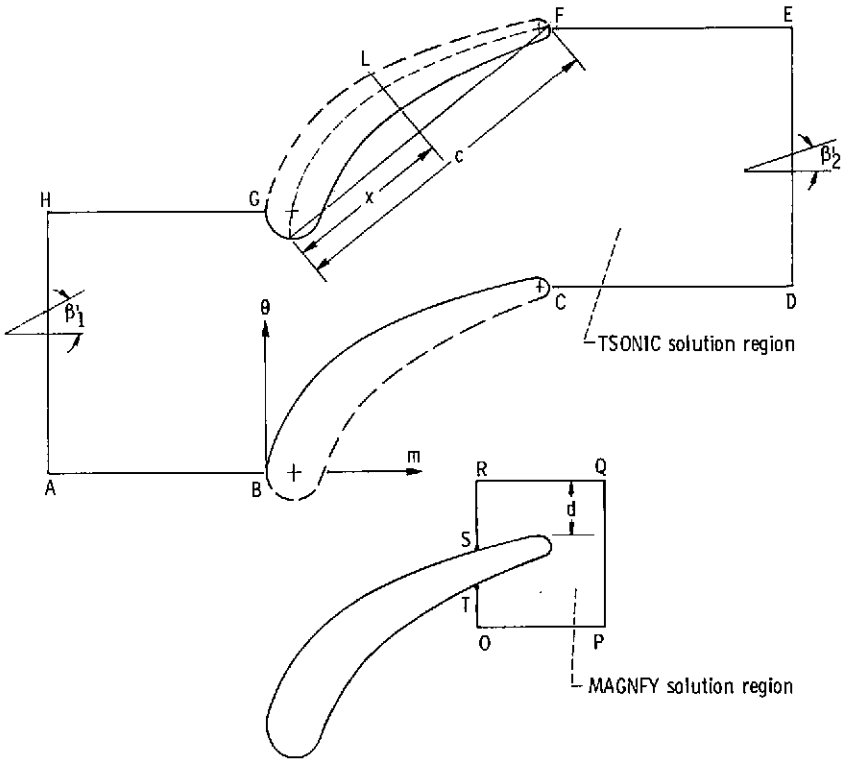

Figure 5. - Solution regions for TSONIC and MAGNFY.

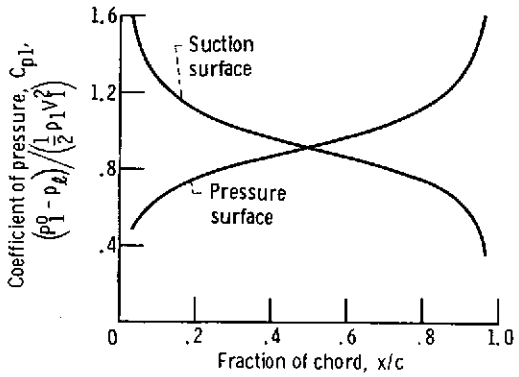

Figure 6. - Pressure distribution for a zero-thickness flat-plate cascade with zero turning calculated by using TSONIC. Inlet flow angle, β_1, 30^0; incidence angle, i, 10^0; deviation angle, δ, 10^0.

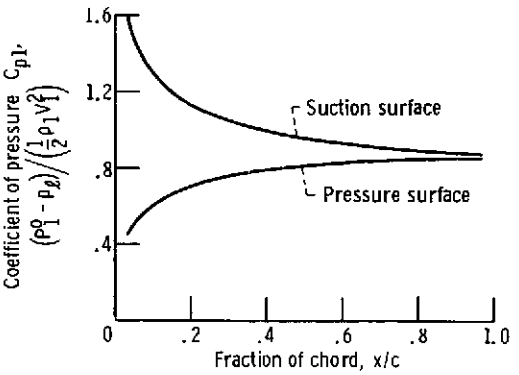

Figure 7. - Pressure distribution for a zero-thickness flat-plate cascade with the Kutta condition satisfied calculated by using TSONIC. Inlet flow angle, β_1, 30^0; incidence angle, i, 10^0; deviation angle, δ, 0.48^0.

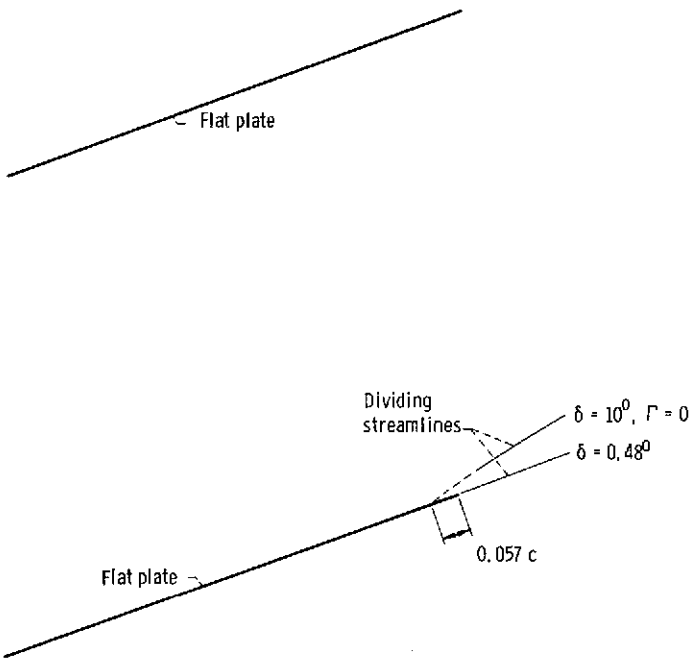

Figure 8. - Dividing streamlines for a zero-thickness flat-plate cascade calculated by using the TSONIC, MAGNFY, and STGPLS programs. Inlet flow angle, β_1, 30^0; incidence angle, i, 10^0; blade solidity, σ, 1.0; blade chord, c, 0.127 meter; Mach number at blade row entrance, M_1, 0.08.

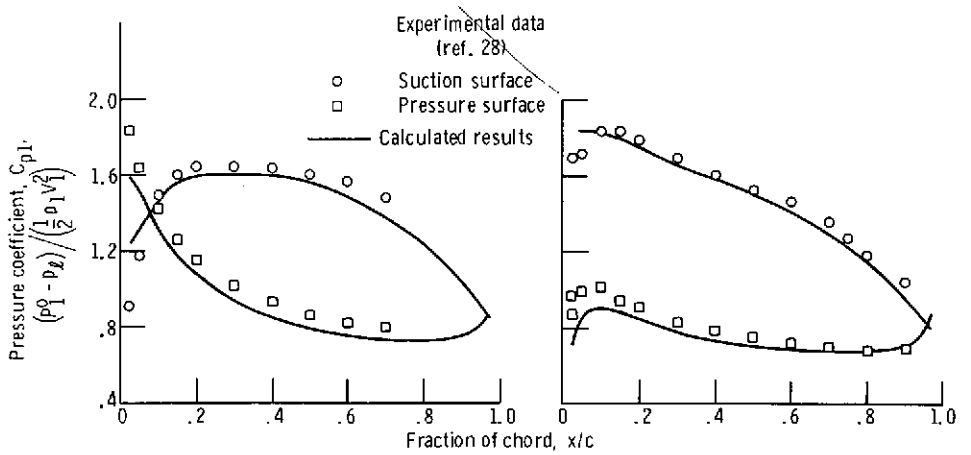

(a) Incidence angle, i, -7.7^0; deviation angle, δ, 8.8^0.

(b) Incidence angle, i, 0.3^0; deviation angle, δ, 8.7^0.

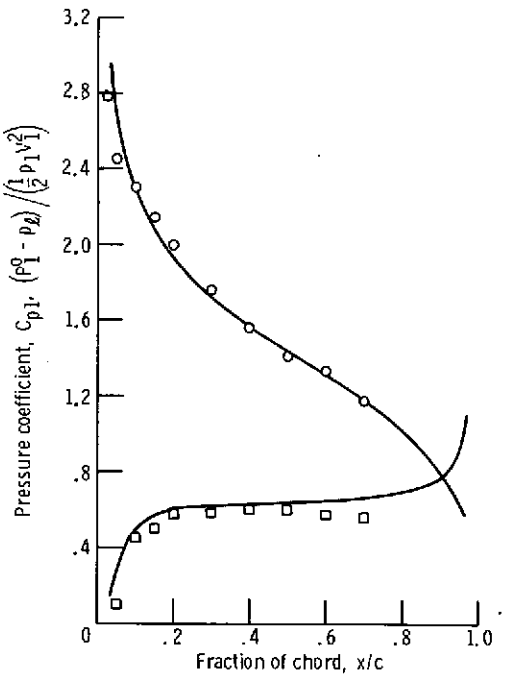

(c) Incidence angle, i, 11.3^0; deviation angle, δ, 12.15^0.

Figure 9. - Comparison of blade surface pressure distributions calculated for a 10C4/30C50 cascade by using experimental deviation angles with measurements from reference 28, for an inlet flow angle β_1 of 30^0. Blade solidity, σ, 1.0.

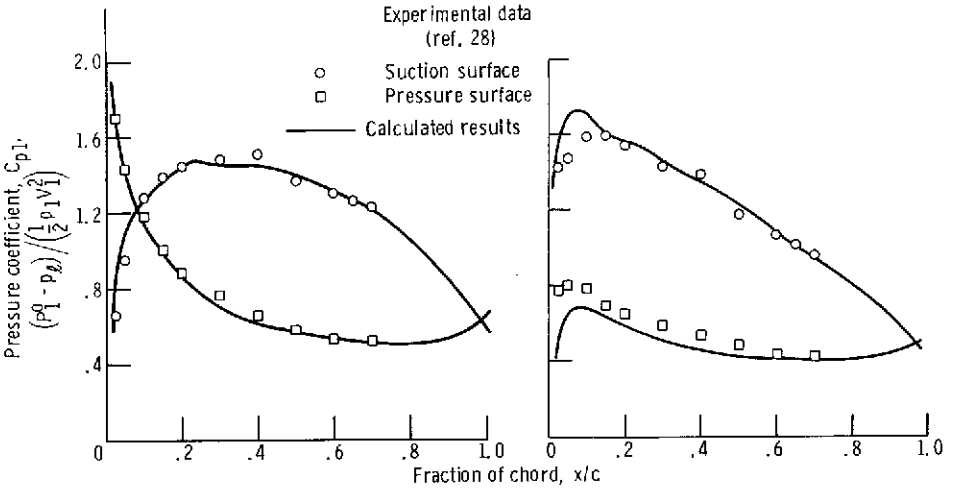

(a) Incidence angle, i, -9.0^0; deviation angle, δ, 10.45^0.

(b) Incidence angle, i, -1.2^0; deviation angle, δ, 11.3^0.

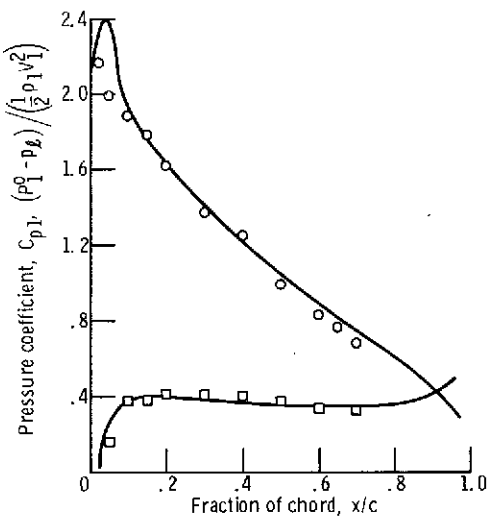

(c) Incidence angle, i, 6.6^0; deviation angle, δ, 14.4^0.

Figure 10. - Comparison of blade surface pressure distributions calculated for a 10C4/30C50 cascade by using experimental deviation angles with measurements from reference 28, for an inlet flow angle β_1 of 60^0. Blade solidity, σ, 1.0.

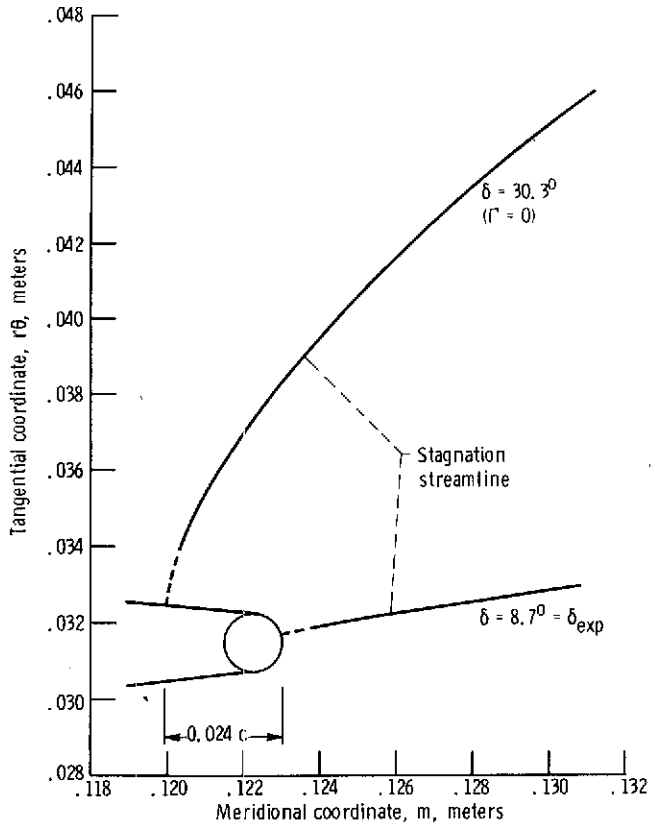

Figure 11. - Stagnation streamlines calculated for a 10C4/30C50 cascade by using experimental deviation angles and zero turning. Inlet flow angle, β_1, 30°; incidence angle, i, 0.3°; blade solidity, σ, 1.0.

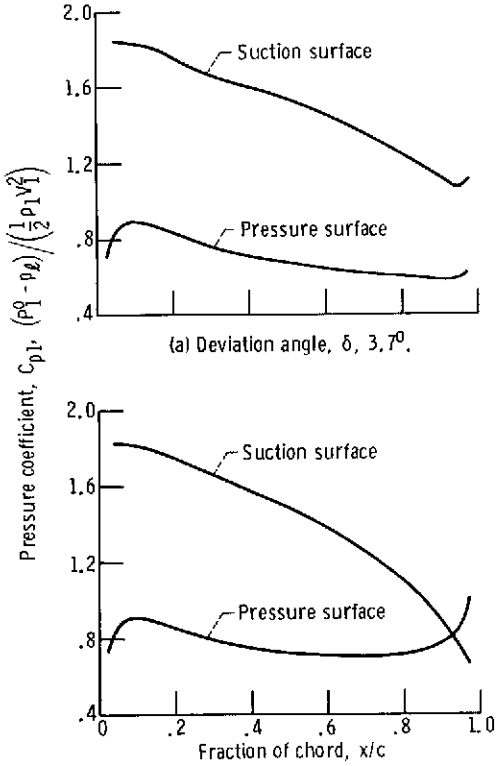

(a) Deviation angle, δ, 3.7°.

(b) Deviation angle, δ, 11.2°.

Figure 12. - Pressure distributions calculated for a 10C4/30C50 cascade by using two deviation angles. Inlet flow angle, β_1, 30°; incidence angle, i, 0.3°; blade solidity, σ, 1.0.

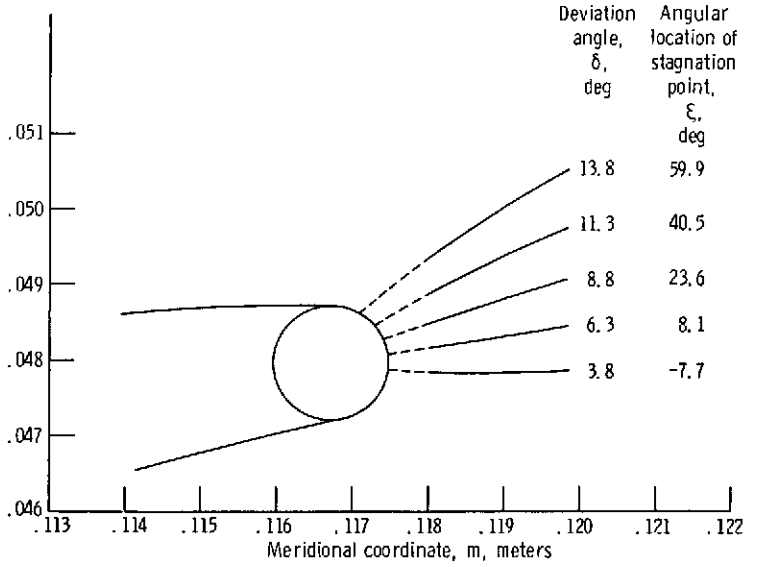

(a) Incidence angle, i, -7.7°.

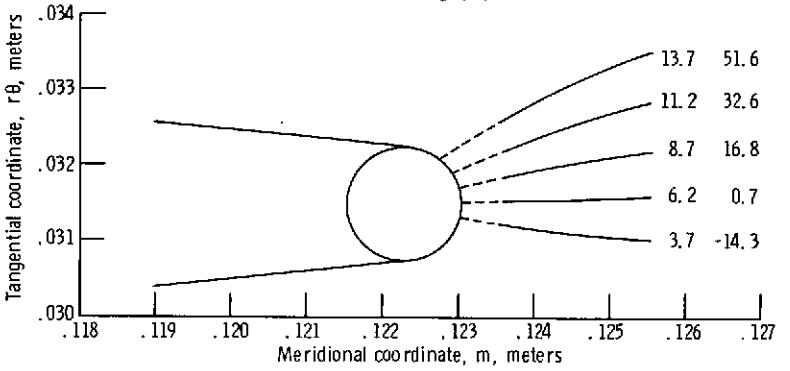

(b) Incidence angle, i, 0.3°.

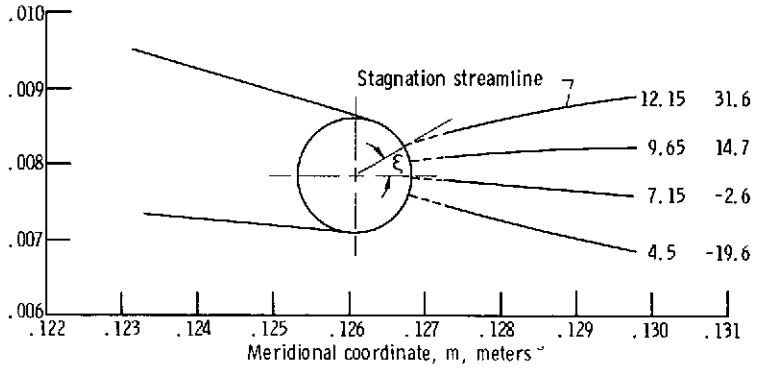

(c) Incidence angle, i, 11.3°.

Figure 13. - Stagnation streamline locations for inviscid-flow solution at several incidence angles. Inlet flow angle, β_1, 30°; blade solidity, σ, 1.0.

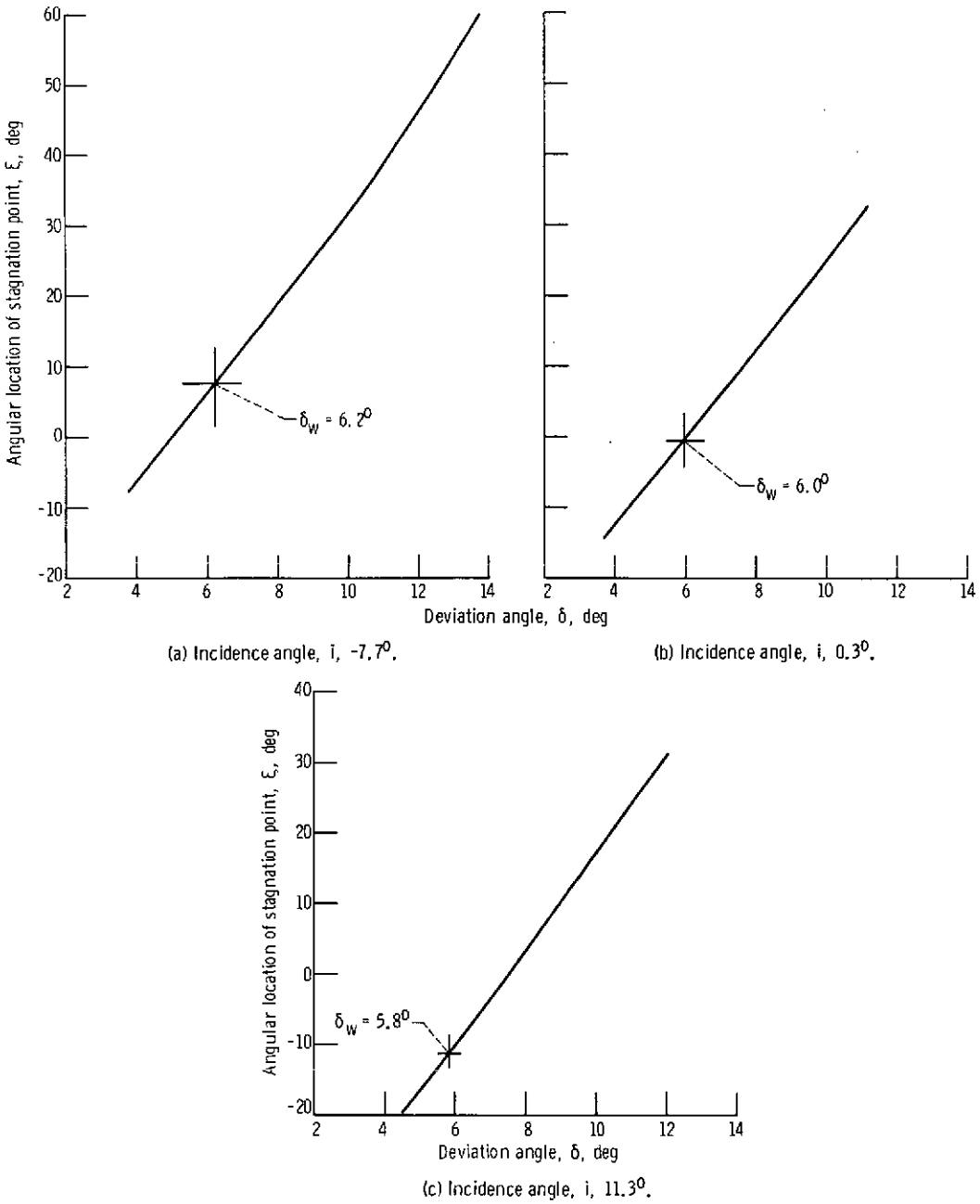

(a) Incidence angle, i, -7.7°.

(b) Incidence angle, i, 0.3°.

(c) Incidence angle, i, 11.3°.

Figure 14. - Deviation angle as function of stagnation point location for a 10C4/30C50 cascade. Inlet flow angle, β_1, 30°; blade solidity, σ, 1.0.

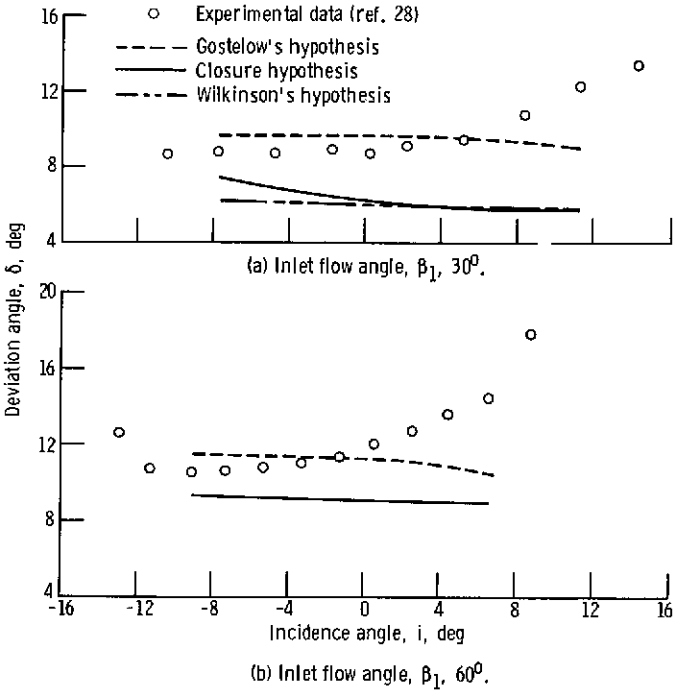

Figure 15. - Comparison of measured and calculated deviation angles for a 10C4/30C50 cascade with a blade solidity σ of 1.0.

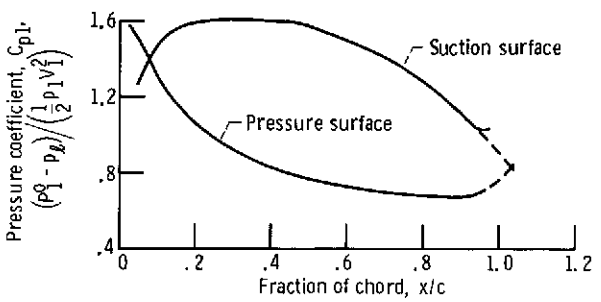

Figure 16. - Example of extrapolation required in applying closure hypothesis. Inlet flow angle, β_1, 30°; deviation angle, δ, 6.3°; blade solidity, σ, 1.0; incidence angle, i, -7.7°.

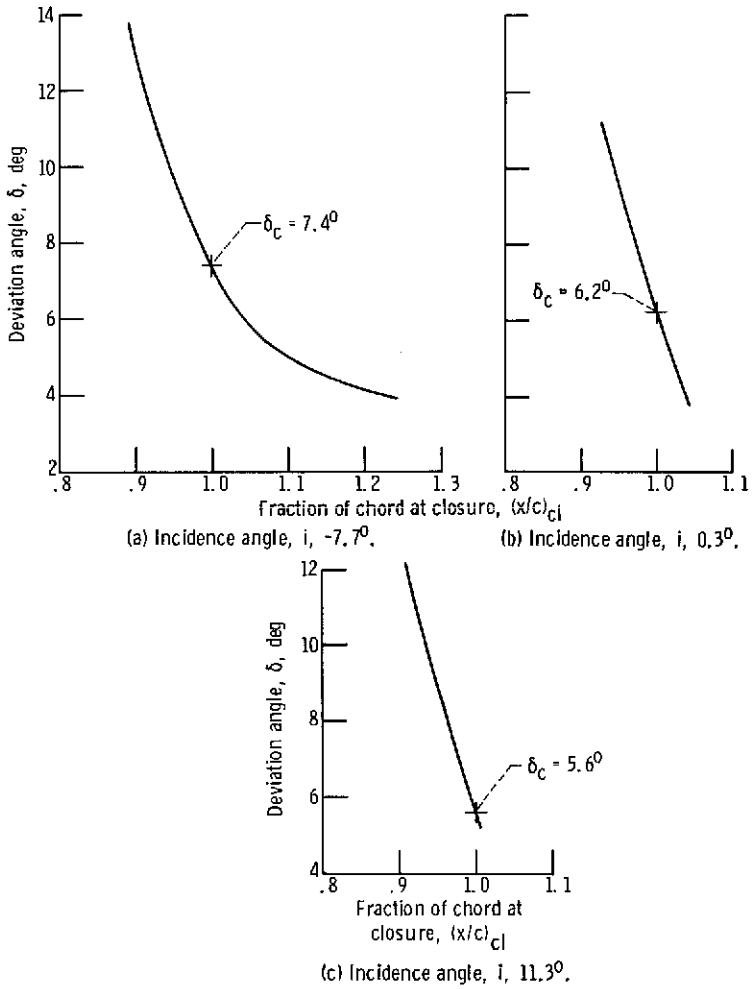

Figure 17. - Relation between closure point of pressure distribution and deviation angle for a 10C4/30C50 cascade, for an inlet flow angle β_1 of 30°. Blade solidity, σ, 1.0.

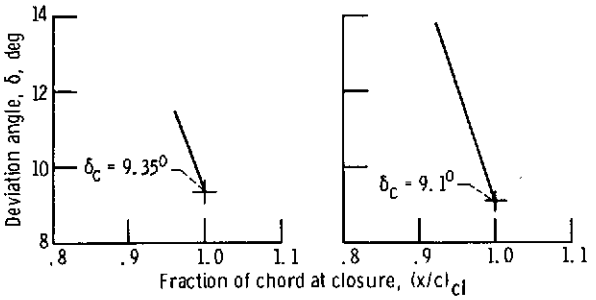

(a) Incidence angle, i, -9.0°. (b) Incidence angle, i, -1.2°.

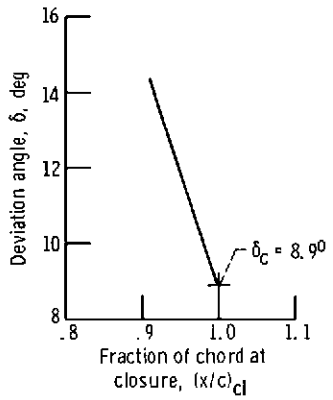

(c) Incidence angle, i, 6.6°.

Figure 18. - Relation between closure point of pressure distribution and deviation angle for a 10C4/30C50 cascade, for an inlet flow angle β_1 of 60°. Blade solidity, σ, 1.0.

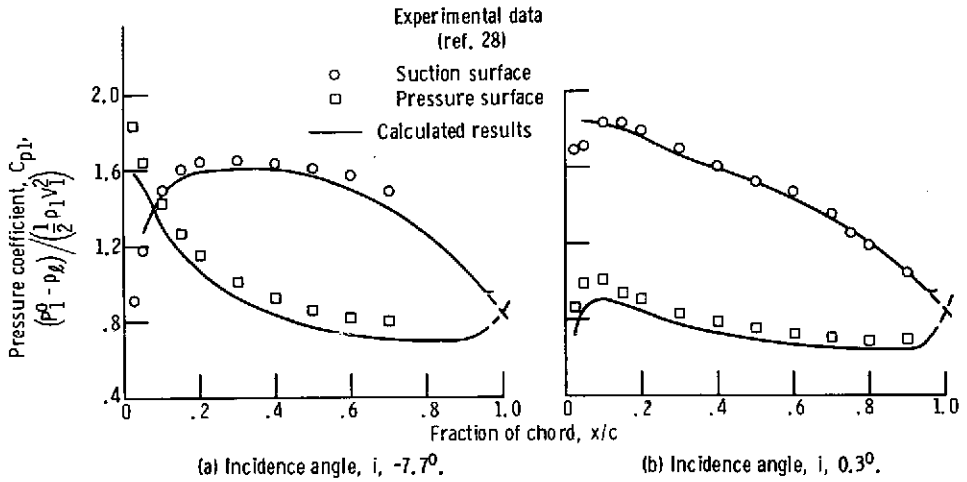

(a) Incidence angle, i, -7.7^0.

(b) Incidence angle, i, 0.3^0.

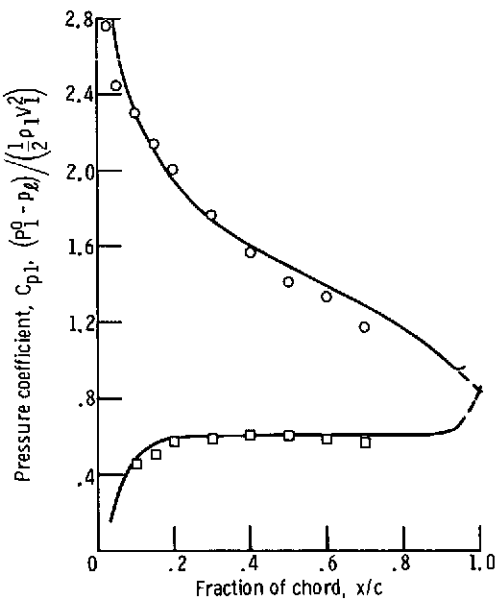

(c) Incidence angle, i, 11.3^0.

Figure 19. - Comparison of pressure distributions calculated by using the closure hypothesis with experimental data for a 10C4/30C50 cascade, for an inlet flow angle β_1 of 30^0. Blade solidity, σ, 1.0.

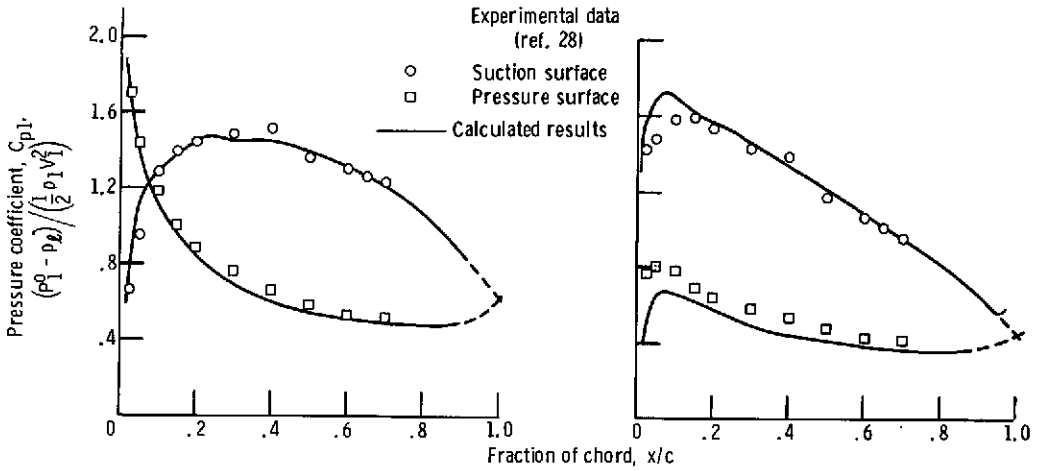

(a) Incidence angle, i, -9.0^0.

(b) Incidence angle, i, -1.2^0.

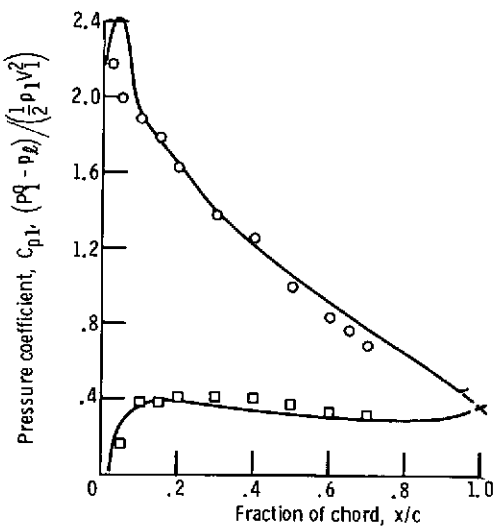

(c) Incidence angle, i, 6.6^0.

Figure 20. - Comparison of pressure distributions calculated by using the closure hypothesis with experimental data for a 10C4/30C50 cascade, for an inlet flow angle β_1 of 60^0. Blade solidity, σ, 1.0.

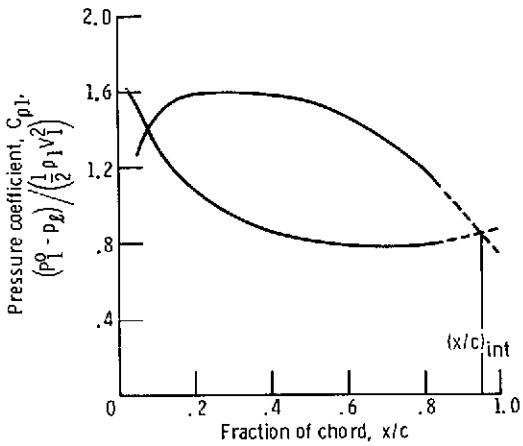

Figure 21. - Linear extrapolation of a calculated pressure distribution for a 10C4/30C50 cascade. Inlet flow angle, β_1, 30^0; deviation angle, δ, 11.3^0; blade solidity, σ, 1.0.

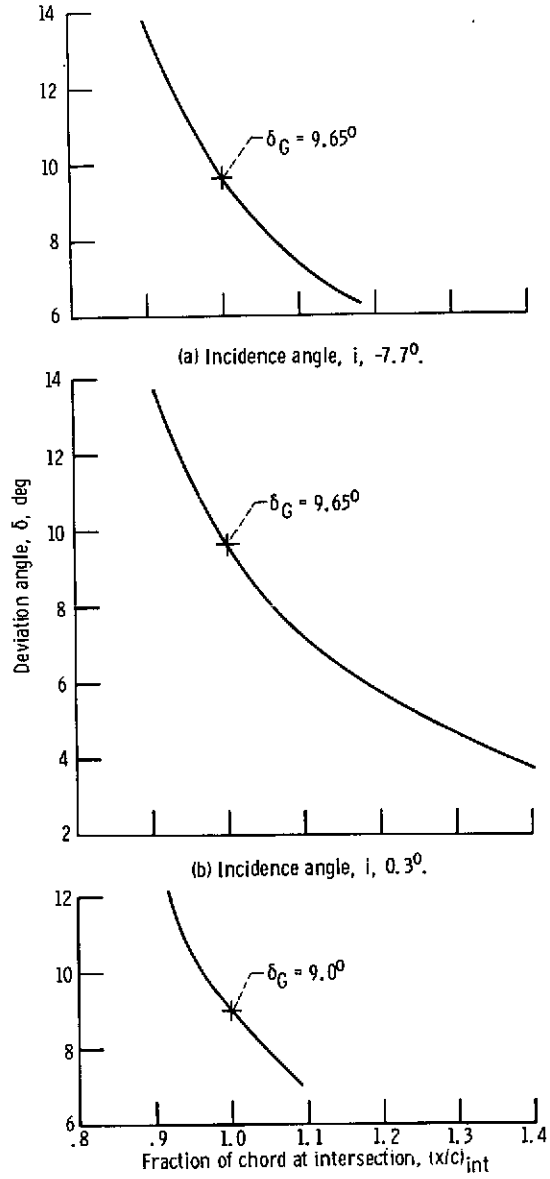

(a) Incidence angle, i, -7.7^0.

(b) Incidence angle, i, 0.3^0.

(c) Incidence angle, i, 11.3^0.

Figure 22. - Relation between deviation angle and point of intersection of linearly extrapolated pressure distributions for a 10C4/30C50 cascade, for an inlet flow angle β_1 of 30^0. Blade solidity, σ, 1.0.

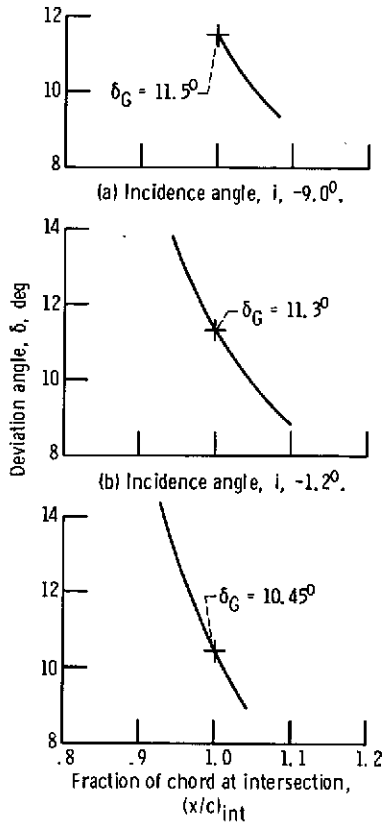

(a) Incidence angle, i, -9.0°.

(b) Incidence angle, i, -1.2°.

(c) Incidence angle, i, 6.6°.

Figure 23. - Relation between deviation angle and point of intersection of linearly extrapolated pressure distributions for a 10C4/30C50 cascade, for an inlet flow angle β_1 of 60°. Blade solidity, σ, 1.0.

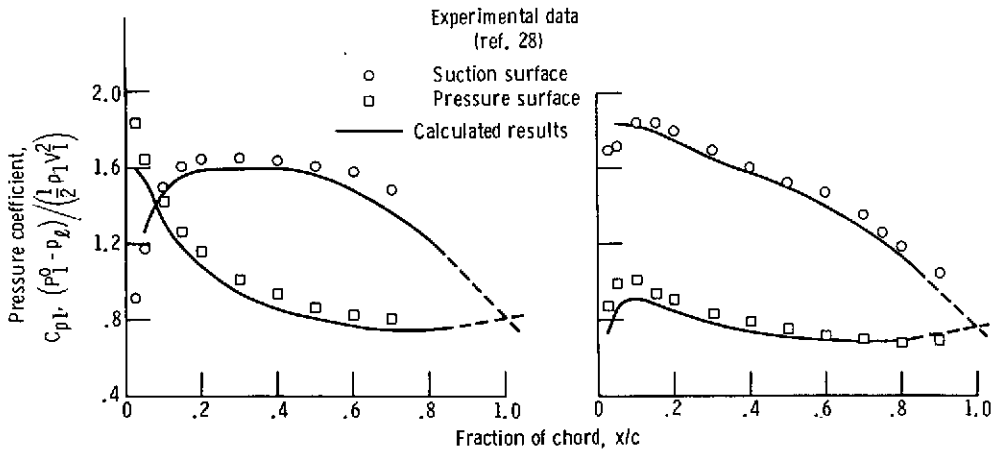

(a) Incidence angle, i, -7.7^0; deviation angle, δ, 9.65^0.

(b) Incidence angle, i, 0.3^0; deviation angle, δ, 9.65^0.

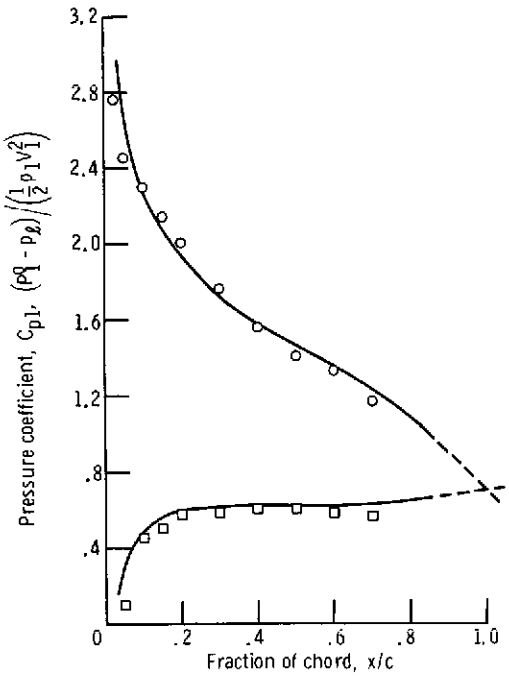

(c) Incidence angle, i, 11.3^0; deviation angle, δ, 9.0^0.

Figure 24. - Comparison of pressure distributions calculated by using Gostelow's hypothesis with experimental data for a 10C4/30C50 cascade, for an inlet flow angle β_1 of 30^0. Blade solidity, σ, 1.0.

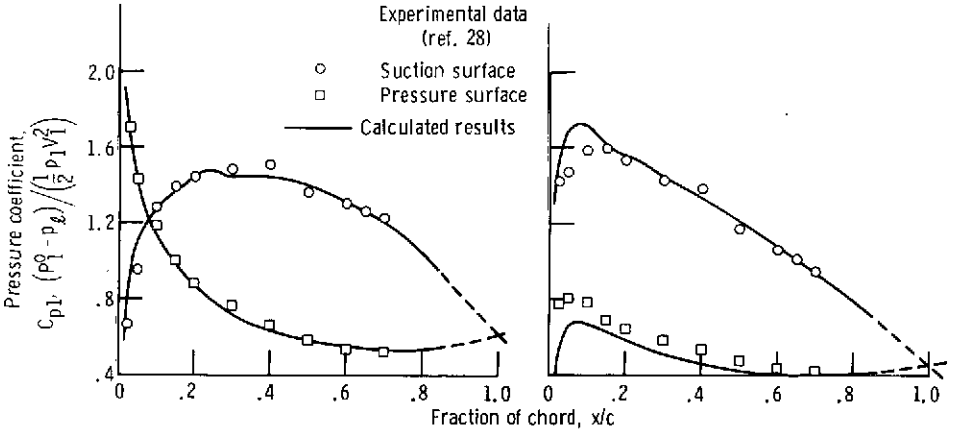

(a) Incidence angle, i, -9.0^0.

(b) Incidence angle, i, -1.2^0.

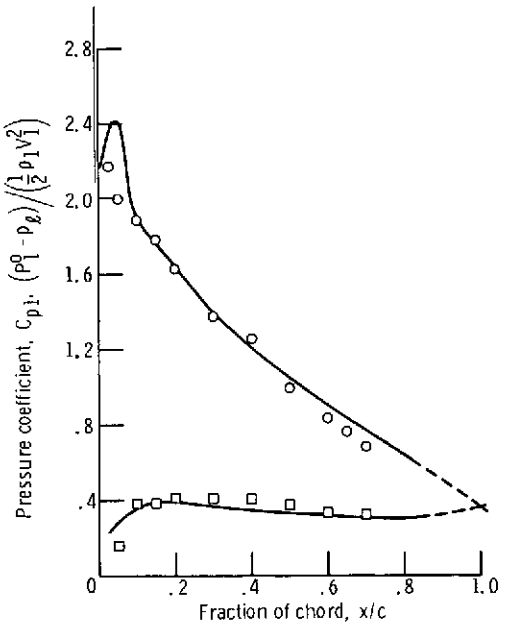

(c) Incidence angle, i, 6.6^0; deviation angle, δ, 10.45^0.

Figure 25. - Comparison of pressure distributions calculated by using Gostelow's hypothesis with experimental data for a 10C4/30C50 cascade, for an inlet flow angle β_1 of 60^0. Blade solidity, σ, 1.0.

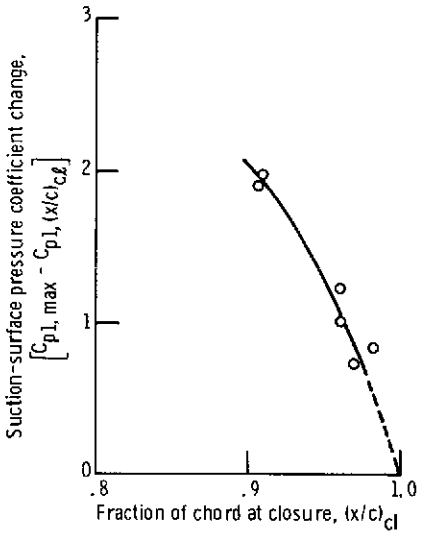

Figure 26. - Relation between closure point of pressure distribution and suction-surface diffusion for a 10C4/30C50 cascade calculated by using experimental deviation angles. Blade solidity, σ, 1.0.

NASA-Langley, 1974 E-7453